Supporting Information

Construction of ZnS-In_2S_3 Nanonests and Its Heterojunction Boosted Visible-light Photocatalytic/Photoelectrocatalytic Performance

Long-Zhen Zhang[a], *Ya-Nan Li*[a], *Minqiang Wang*[a], *Heng Liu*[a], *Hao Chen*[a], *Yanhua Cai*[b], *Tianhao Li*[a], *Maowen Xu*[a] , *Shu-Juan Bao*[a,*]

[a] Key Laboratory of Luminescent and Real-Time Analytical Chemistry (Southwest University), Ministry of Education, Institute for Clean Energy and Advanced Materials, School of Materials and Energy, Southwest University, Chongqing 400715, PR China

[b] Chongqing Key Laboratory of Environmental Materials & Remediation Technologies, Chongqing University of Arts and Sciences, Chongqing 402160, PR China

*Corresponding authors.
E-mail addresses: baoshj@swu.edu.cn (S.J. Bao)

Experimental

0.1 g ZIF-8 and 1.2 g $In(NO_3)_3$•xH_2O were dispersed and mixed in 20 mL ethanol under vigorous stirring. When the milky white suspension became clear, it was transferred it into a 100-mL Teflon-lined stainless-steel autoclave and heated at 120 °C for different hours. After cooling down, the medium products were obtained by filtering.

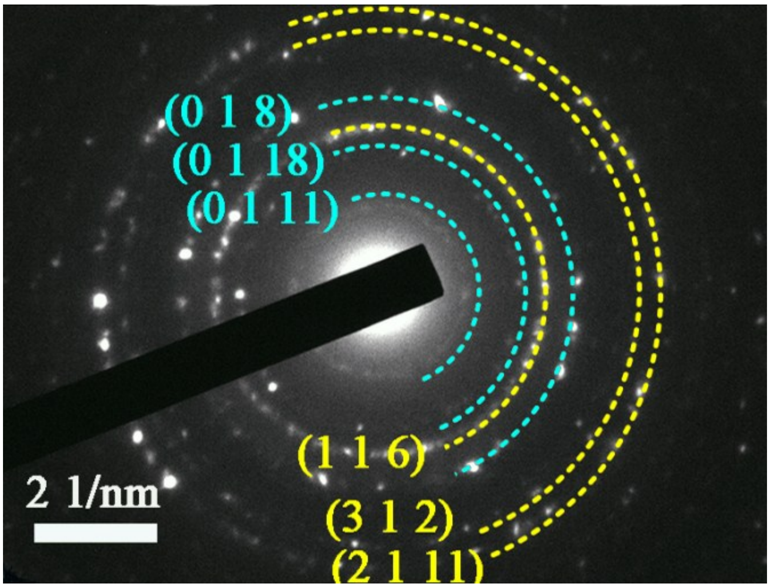

Figure S1 SAED of ZnS-In_2S_3 heterojunction.

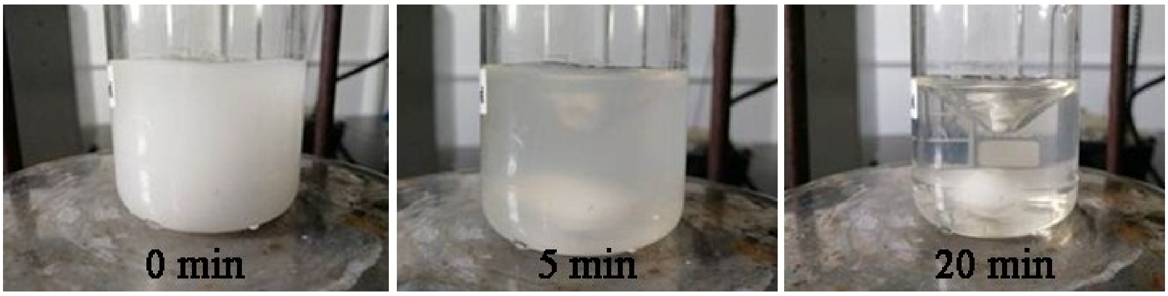

Figure S2 The experimental phenomenon of the initial cation-exchange process with different time.

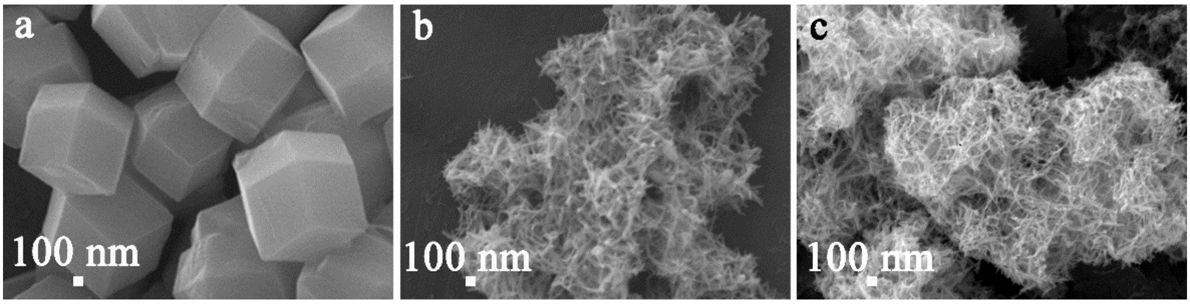

Figure S3 The FE-SEM images of a) ZIF-8, b) medium products of 4 h and c) ZnS-In_2S_3.

As shown in Figure S2 and S3, uniform dodecahedron, ZIF-8, was used as the zinc source (Fig. S3). After a cation-exchange reaction with $In(NO_3)_3$, the milky white ZIF-8 suspension became clear (Fig. S2). After growth for 4 h under solvothermal conditions, a slack network consisting of nanowires was obtained as the intermediate, which is shown in Fig. 3b. After further sulfuration, the product (ZnS-In_2S_3) in Fig. 3c retained a fluffy network structure textured by nanowires, very similar to that of the solvothermal intermedium.

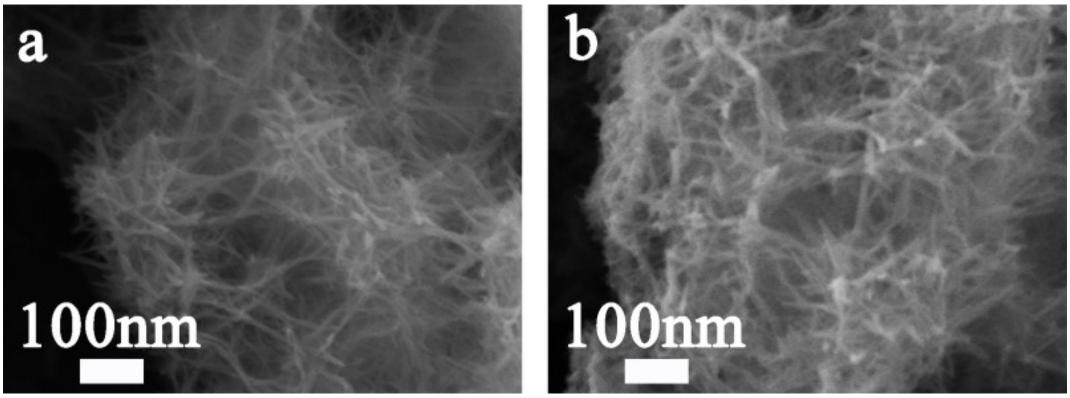

Figure S4 the FE-SEM images of a) medium products of 5 h and b) its corresponding sulfide.

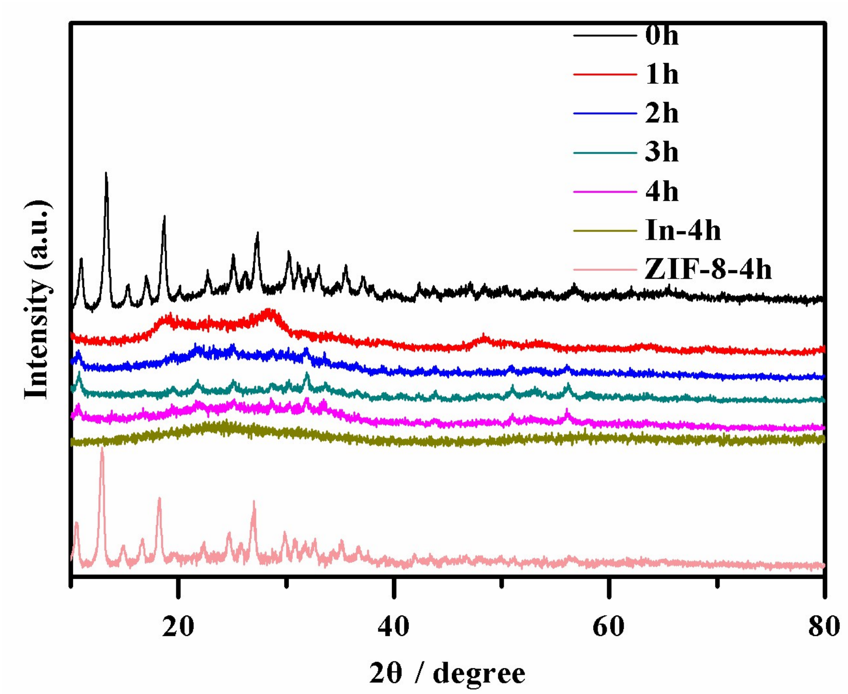

Figure S5 the XRD patterns of medium products.

Table S1 The concentration and mass ratio of Zn and In based on ICP of $ZnS-In_2S_3$

Elements	Measured Concentration	Correction Coefficient	Measured Mass Ratio	Measured Atomic Ratio
Zn	1.236 mg/L	0.998028	10.4288	5.941
In	12.89 mg/L	0.998680		

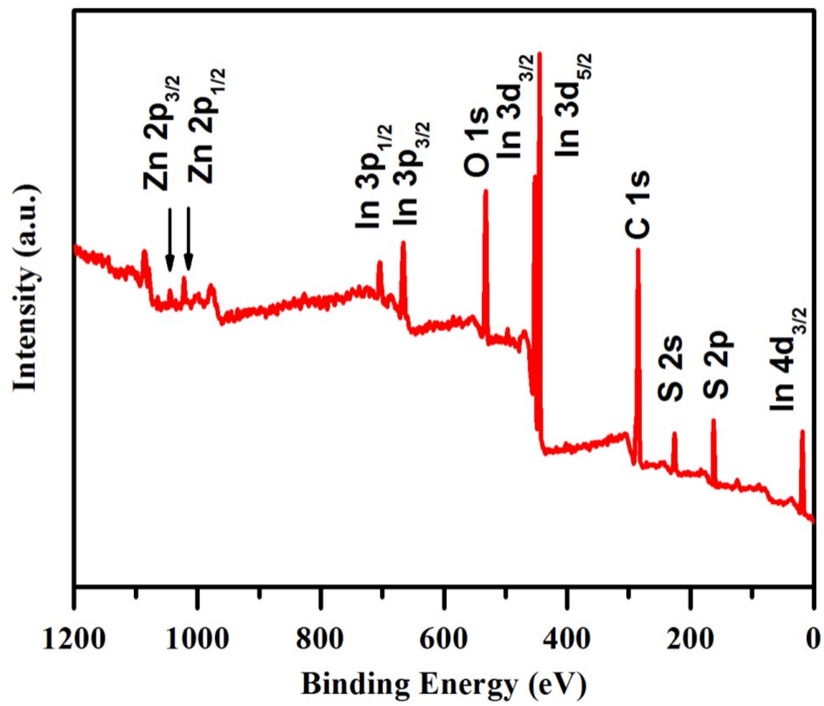

Figure S6 XPS total spectrogram of as-prepared ZnS-In_2S_3 material.

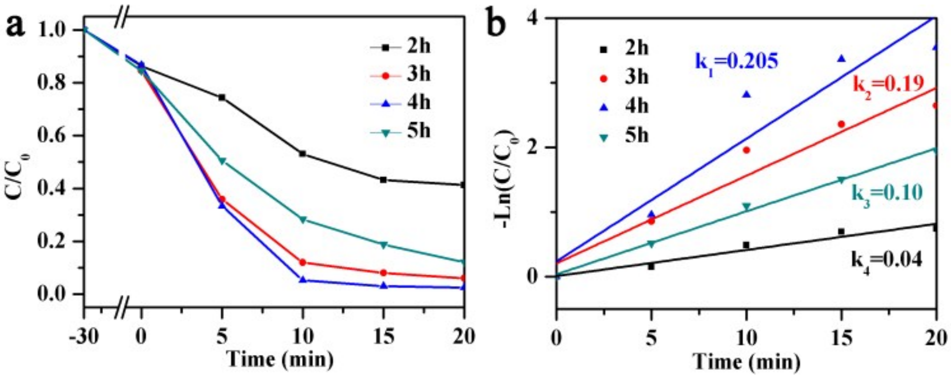

Figure S7 the catalytic performance of the sulfides

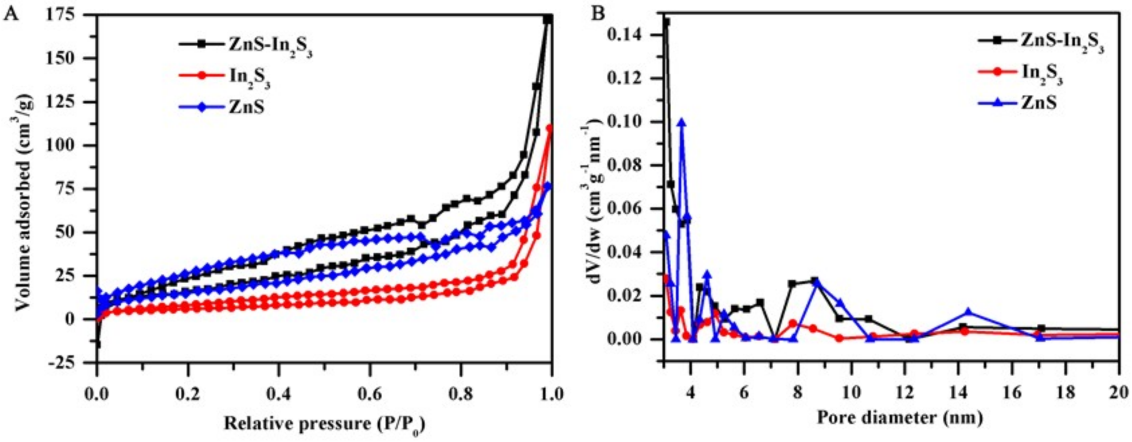

Figure S8 the nitrogen adsorption-desorption isotherms and the corresponding pore size distributions of the as-prepared photocatalysts.

The specific surface areas of ZnS-In_2S_3, In_2S_3 and ZnS are 68.4, 21.2 and 58.8 m^2/g, respectively. And the isotherms of as-prepared photocatalysts are displayed in **Figure S8**.

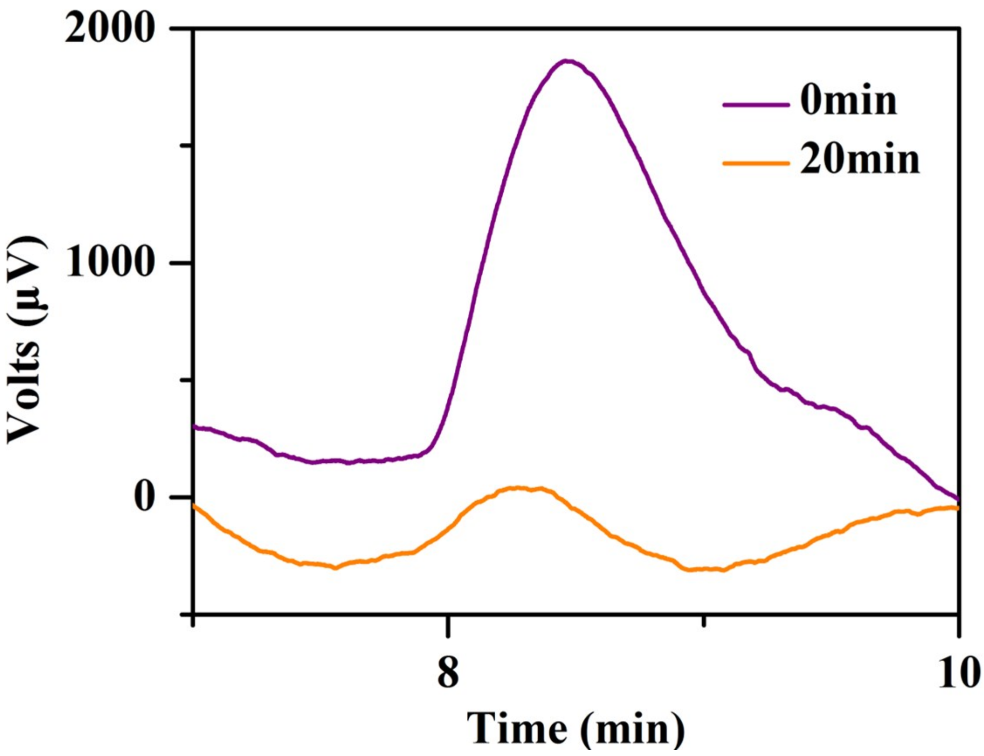

Figure S9. the liquid chromatograms of bisphenol A.

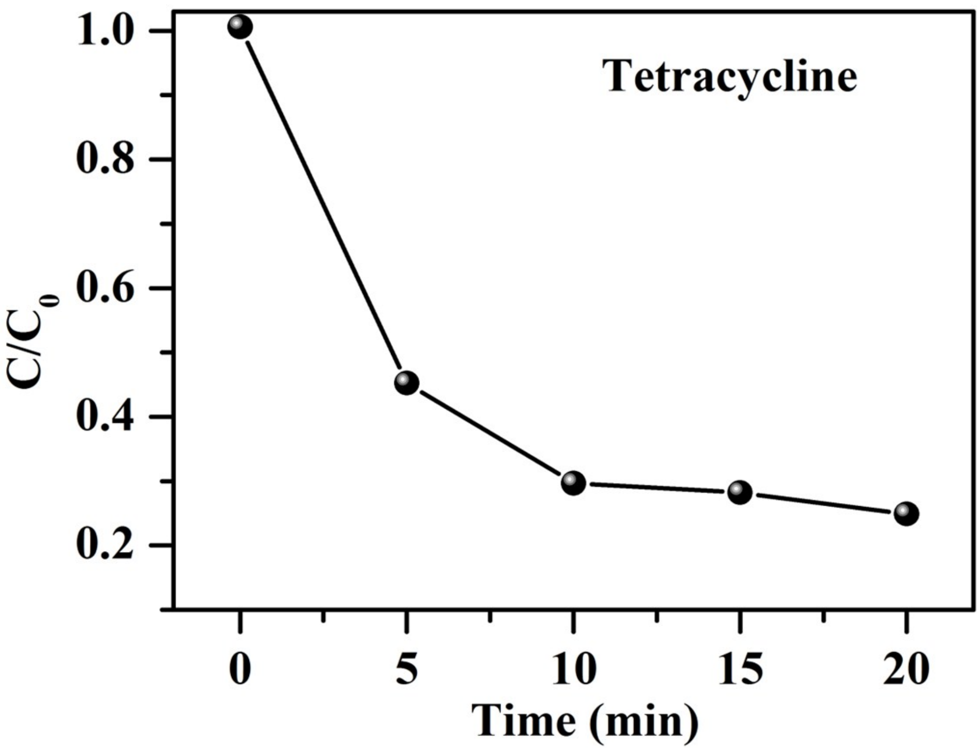

Figure S10. Photocatalytic degradation of tetracycline with time of ZnS-In_2S_3 heterojunction.

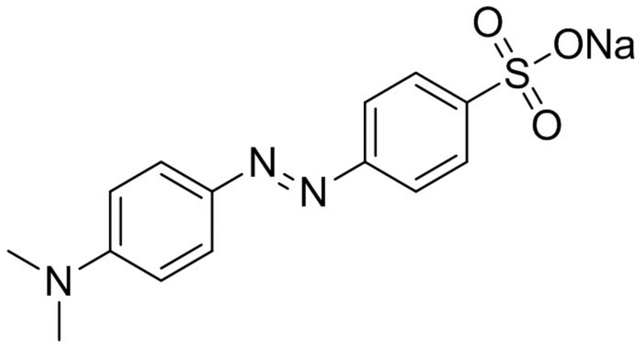

Figure S11. structural formula of MO.

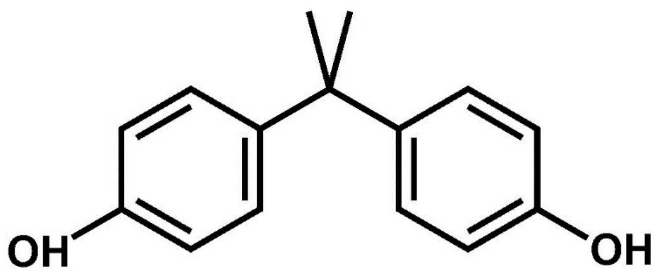

Figure S12. structural formula of BPA.

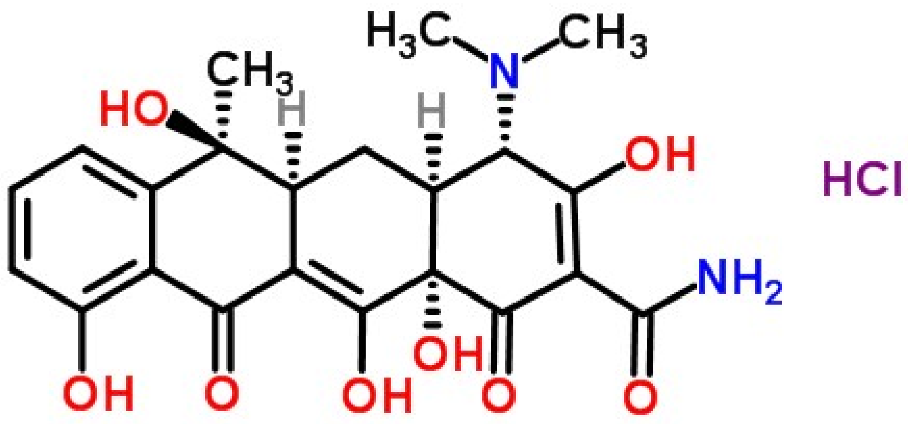

Figure S13. structural formula of TC.

In order to estimate the impact of dye-sensitization on the photocatalytic performance of ZnS-In_2S_3, colorless tetracycline (TC) and bisphenol A (BPA) were chosen as the target pollutant. As shown in **Figure S9** and **S10**, about 73% of TC and 74% of BPA was degraded after a 20-min visible light irradiation. The different degradation rate of TC, BPA and MO should result from their different molecular structure (**Figure S11-S13**), of course, dye photosensitization should also help to increase the degradation efficiency of our designed materials, but the main reason should ascribe to the heterojunction structure of material itself.

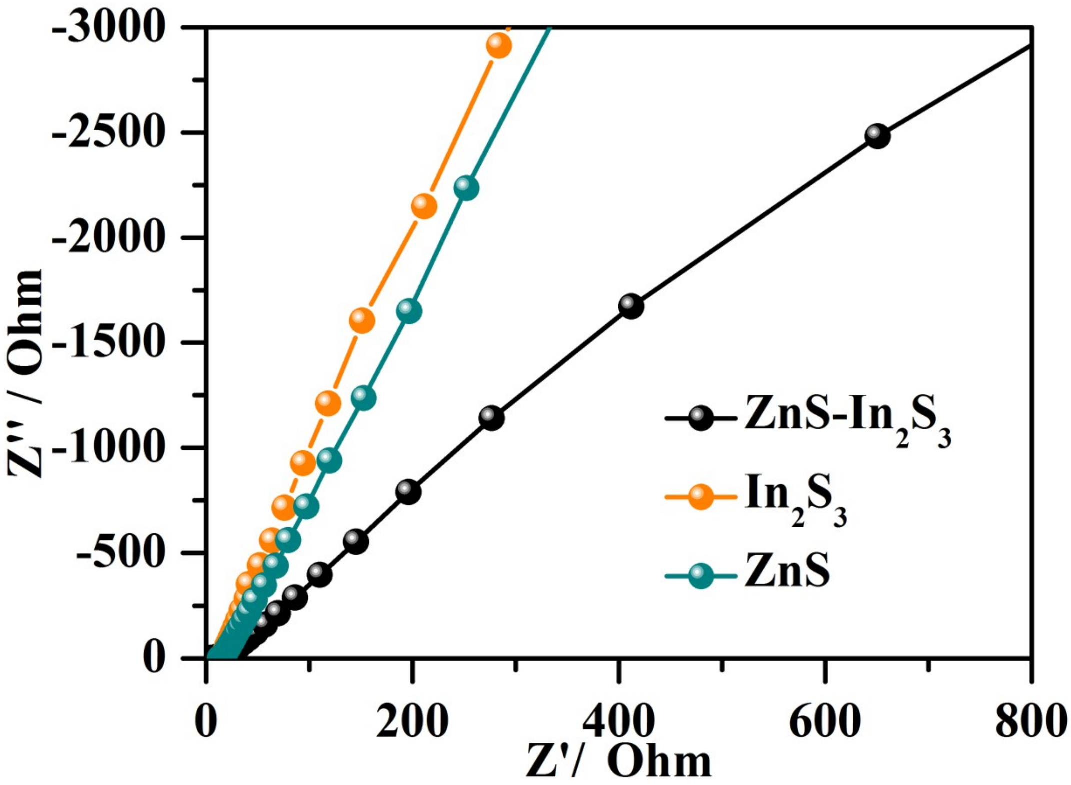

Figure S14. EIS Nyquist plots of $ZnS\text{-}In_2S_3$, In_2S_3 and ZnS samples.

The charge transfer was studied via electrochemical impedance spectroscopy. As Figure S14 shows, the Nyquist plot of $ZnS\text{-}In_2S_3$ heterojunction has a smaller arc radius in comparison to pure ZnS and pure In_2S_3, manifesting the higher electronic conductivity of $ZnS\text{-}In_2S_3$ due to electron transfer between ZnS and In_2S_3. The low charge transfer resistance/high electronic conductivity favored more efficient charge separation, which can also demonstrate the superiority of $ZnS\text{-}In_2S_3$ nanosized heterojunction.

Table S2 Examples of photocatalytic materials employed for MO degradation applications.

Catalysts	Light source	Concentration (ppm)	Time (min)	Degradation rate (%)	Refereces
TiO_2/ZSM-5	550 W Max Lamp	20	180	99.55	1
MIL-100(Fe)-RT	150 W UV lamp	5	420	64	2
PS-C_3N_4	Visible light by a 300 W Xe lamp	10	60	85.85	3
TiO_2	300 W UV light	10	105	~100	4
In_2S_3	Visible light by 500W Xe lamp	10	120	97	5
In_2S_3/$In(OH)_3$	300 W Xe-arc lamp	5	100	~94	6
ZnS-In_2S_3	Visible light by 220W lamp	10	20	98	This work

Reference

1 H. Znad, K. Abbas, S. Hena, M. R. Awual, *J. Environ. Chem. Eng.*, 2018, **6**, 218.

2 K. Guesh, C. A. D. Caiuby, Á. Mayoral, M. Díaz-García, I. Díaz, M.Sanchez-Sanchez, *Crystal Growth Design*. 2017, **17**, 1806.

3 L. Jiang, X. Yuan, G. Zeng, X. Chen, Z. Wu, J. Liang, J. Zhang, H. Wang, H. Wang, *ACS Sustainable Chem. Eng.* 2017, **5**, 5831.

4 J. Chang, W. Zhang, C. Hong, *Chin. J. Chem.* 2017, **35**, 1016.

5 Y. Fang , S. R. Zhu , M. K. Wu, W. N. Zhao, L. Han, *J. Solid State Chem.* 2018, **266**, 205.

6 Z. Qiao, T.Yan, W. Li, B. Huang, *New J. Chem.*, 2017, **41**, 3134.